Materials Science and Engineering B 177 (2012) 127–131

Contents lists available at SciVerse ScienceDirect

Materials Science and Engineering B

journal homepage: www.elsevier.com/locate/mseb

Crystallinity, magnetic and electrochemical studies of PVDF/Co_3O_4 polymer electrolyte

Aarti Sripathi Bhatt, Denthaje Krishna Bhat*

Department of Chemistry, National Institute of Technology Karnataka, Surathkal, Srinivasnagar 575025, India

ARTICLE INFO

Article history:
Received 6 May 2011
Received in revised form
12 September 2011
Accepted 26 September 2011
Available online 25 October 2011

Keywords:
Nanocomposites
PVDF
Co_3O_4
Crystallinity
Magnetic properties
Conductivity

ABSTRACT

Organic–inorganic nanocomposites are gaining importance in the recent times as polymer electrolyte membranes. In the present work, composites were prepared by combining nano sized Co_3O_4 and poly(vinyledene fluoride) (PVDF), using spin coating technique. The surface of the PVDF/Co_3O_4 system characterized through field emission scanning electron microscopy (FESEM) revealed a porous structure of the films. The nanoparticles tend to aggregate on the surface and inside the pores, leading to a decrease in the porosity with an increase in Co_3O_4 content. Co_3O_4 nanoparticles prohibit crystallization of the polymer. Differential scanning calorimetry (DSC) studies revealed a decrease in crystallinity of PVDF/Co_3O_4 system with an increase in the oxide content. Magnetic property studies of the composite films revealed that with an increase in Co_3O_4 content, the saturation magnetization values of the nanocomposites increased linearly, showing successful incorporation of the nanoparticles in the polymer matrix. Further, ionic conductivity of the composite films was evaluated from electrochemical impedance spectroscopy. Addition of Co_3O_4 nanoparticles enhanced the conductivity of PVDF/Co_3O_4 system.

1. Introduction

Polymer nanocomposites are a result of the combination of polymers and organic/inorganic fillers at the nanometer scale. The extraordinary versatility of these new materials springs from the large selection of polymers and fillers available to researchers. The unique electronic, magnetic and optical properties of nano-fillers enhance the thermal and mechanical properties of the macromolecular material [1].

In the recent years, there is a thrust for solid polymer electrolytes (SPEs) with high ionic conductivity, good electrochemical stability, large transport number and good mechanical strength. Poly(ethylene oxide) (PEO)-based polymer electrolytes are extensively studied in this regard with lithium salts as fillers [2–4]. Lately, polyvinylidene fluoride (PVDF) has become a favorable choice as polymer matrix for SPEs and gel polymer electrolytes (GPEs) due to its appealing properties such as high dielectric constant ($\varepsilon \approx 8.4$) and strong electron withdrawing functional groups (–C–F) [5–8]. In addition, PVDF is stable against most corrosive chemicals and organic compounds including acids, alkalines, strong oxidants and halogens [9,10].

There are reports on the addition of metal oxides like titania (TiO_2) [11], $BaTiO_3$ [12,13] and several lithium salts [6] to understand the electrochemical properties of SPEs. However, the electrochemical and magnetic interactions of cobalt oxide (Co_3O_4) nanoparticles on PVDF matrix have been studied rather rarely. It will be interesting to study what happens when the properties of Co_3O_4 nanoparticles and PVDF blend together.

Here, we make an attempt to examine the effect of Co_3O_4 nanoparticles on the porosity and crystallinity of PVDF matrix and how these two factors help in improving the magnetic property and overall conductivity of PVDF/Co_3O_4 system.

2. Experimental

PVDF (M_w = 275,000) was purchased from Sigma Aldrich and was used in a pellet form. 2% Acetic acid solution was used as a solvent. All chemicals used in the synthesis of Co_3O_4 were used as received. Distilled water was used throughout the experiment.

2.1. Synthesis of Co_3O_4

Co_3O_4 naoparticles were synthesized by microwave method. The exact procedure is described elsewhere [14]. In brief, Co_3O_4 nanoparticles of average diameter 6 nm were prepared by subjecting the cobalt salt solution to microwave irradiation. The surfactant trioctyl phosphine oxide (TOPO) was used to control the size.

* Corresponding author. Tel.: +91 824 2474000x3202; fax: +91 824 2474033.
E-mail address: denthajekb@gmail.com (D.K. Bhat).

0921-5107/$ – see front matter © 2011 Elsevier B.V. All rights reserved.
doi:10.1016/j.mseb.2011.09.036

2.2. Preparation of PVDF–Co_3O_4 nanocomposite films

Desired amounts of PVDF polymer pellets were added to DMF and subjected to vigorous shaking to ensure thorough wetting of the polymer pellets. The mixture was kept in a sonicator maintained at 60 °C. After complete dissolution of polymer pellets, required amount of Co_3O_4 additive was added and sonication was continued till the nanoparticles dispersed homogeneously in the polymer solution. The solutions were then spin coated (Spin-Coater ACE-1020 Series) on a glass substrate at 500 rpm, 1000 rpm and 2000 rpm for 60 s sequentially. The glass substrate was then immediately immersed in distilled water for 24 h to ensure complete removal of residual solvent. Under similar condition, a blank PVDF film was also prepared. The films were labeled as PC0, PC1, PC2, PC3 and PC4 for Co_3O_4 content of 0, 0.3, 0.5, 0.7 and 1 wt.%, respectively. Addition of Co_3O_4 content higher than 1 wt.% leads to a heterogeneous solution.

2.3. Characterization

A Zeiss SUPRA 40VP Gemini field emission scanning electron microscope (FESEM) was used to analyze the surface morphologies of the polymer electrolytes. The films were gold coated using a sputter coating operated under vacuum. The porosity of the polymer electrolyte membranes were measured by immersing the membrane in *n*-butanol for 2 h after which the membrane surface was dried with a filter paper. The polymer sample of dimension 1 cm × 1 cm and thickness in the range of 80–100 μm were taken. The membranes were weighed before and after the absorption of *n*-butanol. The porosity was calculated using the following equation:

$$P\% = \frac{M_b/\rho_b}{(M_p/\rho_p) + (M_b/\rho_b)} \quad (1)$$

where $P\%$ is the porosity of membranes, M_p is the mass of the membrane, M_b is the mass of the absorbed *n*-butanol, ρ_p is the density of the membrane and ρ_b is the density of *n*-butanol. The membrane density was determined by measuring the volume and the weight of membrane. Differential scanning calorimetry (DSC) data was obtained in the temperature range of 35–250 °C (DSC-60, Shimadzu, Japan). The samples, sealed in an aluminum pan, were heated at a rate of 10 °C/min under nitrogen atmosphere. An empty pan was used as reference. The magnetic properties were assessed with a Vibration Sample Magnetometer (ADE-DMS EV-7VSM). Electrochemical impedance measurements were carried out using an electrochemical work station, AUTOLAB 30. The films were placed in between two circular stainless steel electrodes of length 2 cm and the whole set up was held tightly with a plastic clamp (refer Supplementary Material 1). 1 M KOH solution was used as electrolyte. The measurements were carried out using a small amplitude AC signal of 10 mV over a frequency range of 100 kHz to 0.01 Hz at room temperature. In order to ensure the conductivity data, the impedance measurements were taken thrice.

3. Results and discussions

3.1. Morphology

The porous surface of the blank film and composite films was demonstrated by FESEM images (Fig. 1). As can be seen from the FESEM images, addition of Co_3O_4 particles higher than 0.5 wt.%, led to an aggregation on the surface and inside the pores of the polymer membranes. Although a polymer membrane with uniform distribution of Co_3O_4 particles was intended, aggregations of Co_3O_4 particles could not be avoided due to their increasing quantity and nanosize effect. The presence of TiO_2 particles also influenced the pore size of PVDF/$LiClO_4$/TiO_2 membrane films in a similar fashion [11]. The influence of Co_3O_4 nanoparticles on the pore size of the polymer membranes was further quantified from porosity results.

Table 1
Porosity, enthalpy, % crystallinity and magnetization values for PVDF/Co_3O_4 films.

Sample	Porosity (%)	Enthalpy (J g^{-1})	Crystallinity (%)	Ms (emu/g)
PC0	62.39	71.54	100.00	–
PC1	52.37	64.20	61.32	0.022
PC2	49.52	64.05	61.17	0.046
PC3	44.75	57.82	55.22	0.109
PC4	36.54	55.53	53.04	0.139

3.2. Porosity measurements

Porosity of polymer membranes has been reported as one of the important parameters in lithium batteries as it dominates the conduction properties of the carriers [15,16]. Moreover, the porous structure of these membranes play an essential role in oil/water separation [17], membrane absorption or stripping [18] and membrane distillation [19]. The additive being here Co_3O_4, porosity is expected to be one of the dominating factors in the conduction properties of the membrane as a whole [20]. The porosity measurements (Table 1) showed a decrease in the porosity of PVDF/Co_3O_4 system with an increase in the Co_3O_4 nanoparticles content. At a Co_3O_4 content of 1 wt.%, the minimum value is 28.54%, while for blank polymer film, the porosity has a maximum value of 52.37%. The decrease in porosity of PVDF/Co_3O_4 system with increase in Co_3O_4 content, suggests a possible interaction between Co_3O_4 and PVDF [21,22]. Also, as seen in the FESEM images, the extrusion of Co_3O_4 nanoparticles on the porous structure and the aggregation of Co_3O_4 nanoparticles in the inside of the pores with increasing Co_3O_4 content may also influence the porosity of the polymer membranes.

3.3. DSC analysis

The thermal behaviors of the PVDF/Co_3O_4 films were investigated by DSC and thereby, the percentage crystallinity was evaluated. Fig. 2 displays the DSC thermograms for the blank PVDF and PVDF/Co_3O_4 composite films. A main melting peak around 166 °C is observed for each system. By assuming that pure PVDF is 100% crystalline, the relative percentage of crystallinity was calculated using the following equation:

$$\%\,\text{crystallinity} = \frac{\Delta H}{\Delta H^0} \times 100\% \quad (2)$$

Here, PVDF being in β phase (as seen from infra-red spectroscopy, Supplementary Material 2), heat of fusion, ΔH^0, of pure PVDF was taken as 104.7 J g^{-1} [23], ΔH is the heat of fusion of PVDF/Co_3O_4 electrolyte membrane. The latter is obtained by the DSC data. ΔH and % crystallinity for all the samples are listed in Table 1. From Fig. 2 and Table 1, it can be seen that ΔH and % crystallinity decreased with increase in Co_3O_4 content. This may be attributed to the partial inhibition effect of Co_3O_4 addition on the polymer crystal formation. Similar behavior was observed for systems with Fe_3O_4 on PVDF [24] and TiO_2 [4], γ-$LiAlO_2$ [25], Sm_2O_3 [26], lithium salts [27] and ceramic additives [28] on PEO-based electrolyte systems. Also, there may be some complicated interactions between cobalt and oxygen in Co_3O_4 and fluorine in PVDF which may induce structural modifications in the polymer chain such as breaking of the preformed crystals. This renders the polymer amorphous to some extent, favoring the improvement in its conductivity [29].

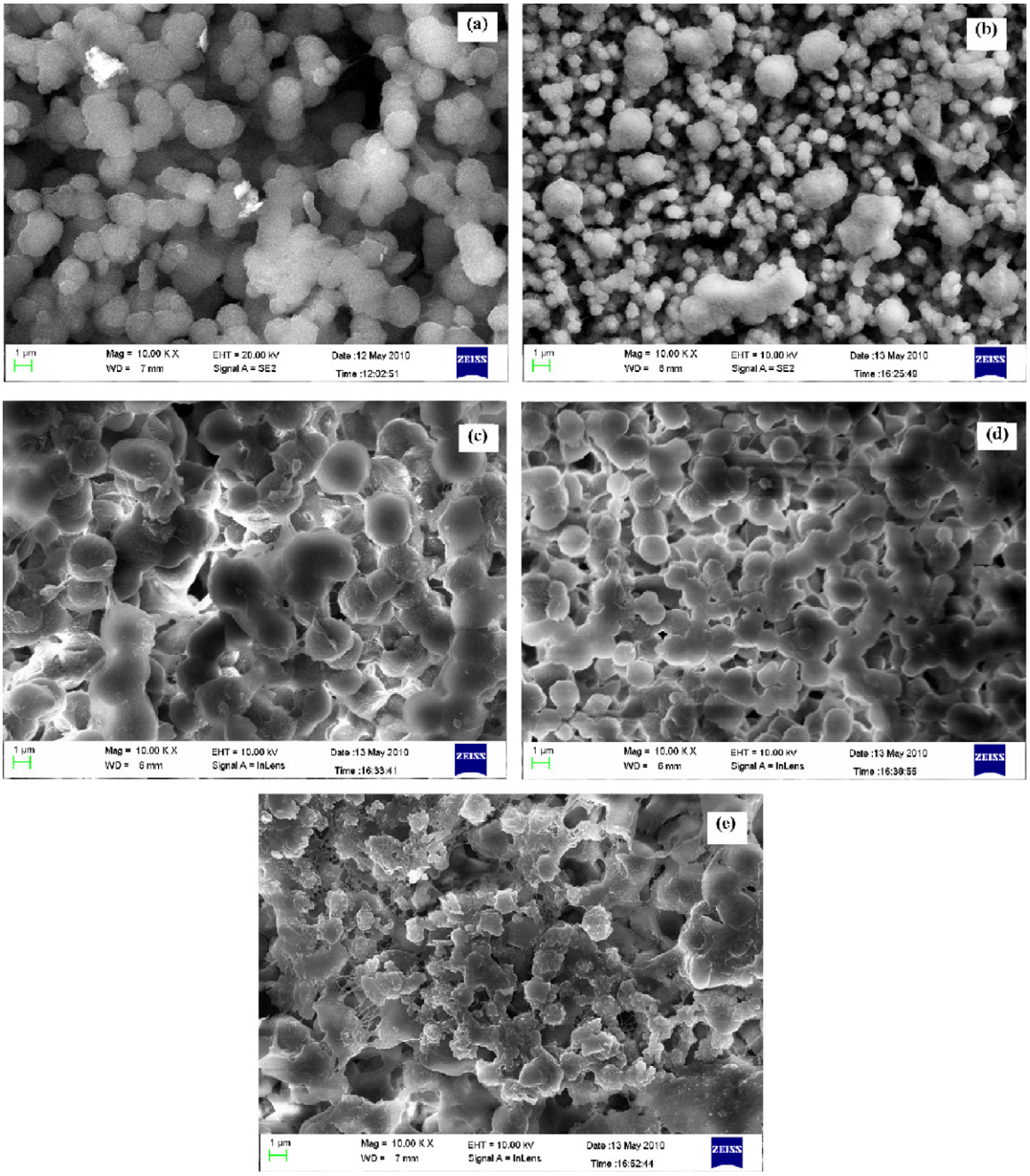

Fig. 1. FESEM images of (a) PC0, (b) PC1, (c) PC2, (d) PC3 and (e) PC4.

3.4. Magnetic measurements

Cobalt oxide in its bulk form is antiferromagnetic and has zero net magnetization. However, in the case of nano sized Co_3O_4 particles, it may happen that because of the uncompensated surface spins and/or finite size effect, they exhibit ferromagnetism [30]. In the present case too, Co_3O_4 nanoparticles displayed a ferromagnetic behavior [14]. Taking advantage of the ferromagnetic nature of these nanoparticles, they were incorporated into the nonmagnetic PVDF polymer matrix. This rendered the composite films magnetic to a certain extent. Fig. 3 shows the variation in magnetization for the composite films as a function of applied field. The magnetization follows a hysteresis curve and gets saturated at a higher field for each of the films (Fig. 3 inset). An unclosed hysteresis loop for PC4 indicates a low magnetization of PC4 at −17,000 Oe. Saturation magnetization (M_s) is a characteristic property of ferromagnetic materials and gives an idea on the extent of ferromagnetism in the material. It is the maximum induced magnetic moment that can be obtained in a magnetic field beyond which no further increase in magnetization occurs. Apparently, the M_s values of the composite films increased with an increase in the content of magnetic nanoparticles (Table 1). This showed that each of the magnetic Co_3O_4 grain contributed to the overall magnetism of the nanocomposite films.

3.5. Conductivity

A polymer electrolyte with high ionic conductivity is very important in practical applications. Ion conduction has been shown to take place in the amorphous phase. Hence, in many

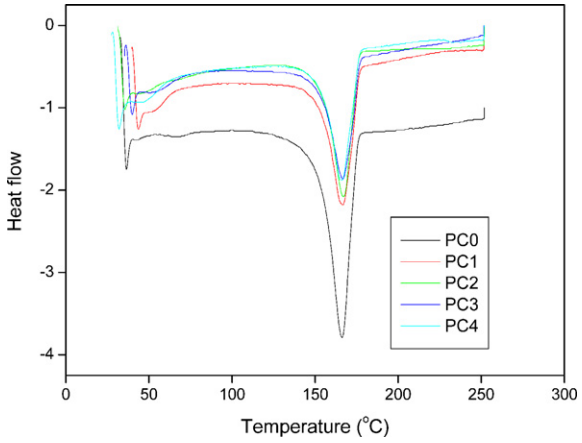

Fig. 2. DSC thermograms of PVDF/Co_3O_4 films.

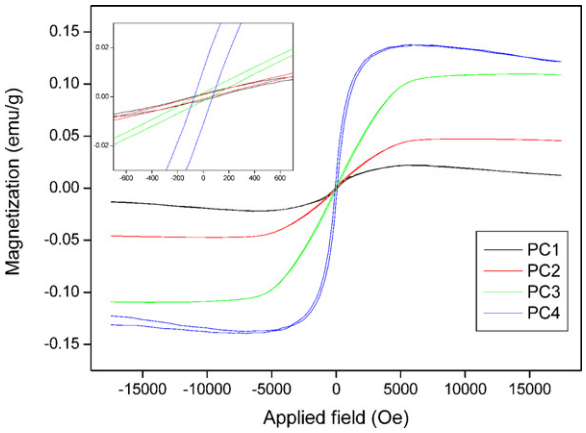

Fig. 3. Room temperature magnetization curves of PVDF/Co_3O_4 films. Inset shows the magnification of the hysteresis loop.

polymer-based electrolytes, the main aim is to limit the crystallinity of the system. One way of increasing the "amorphicity" of the polymer system is to introduce small amount of nano-size particles which disturb the local crystal field and suppress the order [31].

In the present work, the conductivity of the prepared films was studied by electrochemical impedance spectroscopy measurements. Fig. 4 shows the Nyquist plots for PVDF films with Co_3O_4 content of 0 wt.% and 1 wt.%, wherein the dominance of oxide nanoparticles in the electrolyte can be clearly demarcated. The

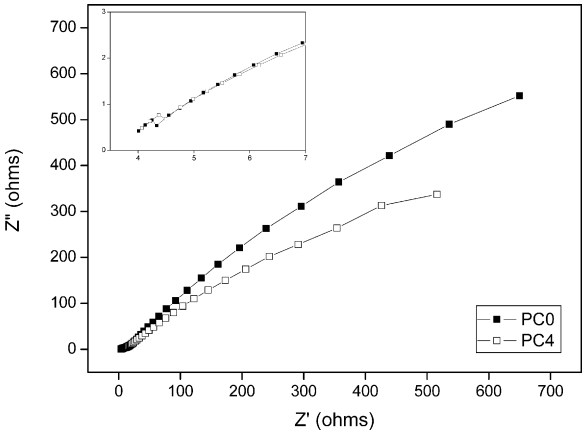

Fig. 4. Nyquist plots of PC0 and PC4. Inset shows the magnification of the Nyquist plots.

charge transfer resistance (R_{ct}) values, obtained by fitting these plots, are $3.154 \times 10^3\ \Omega$ and $2.408 \times 10^3\ \Omega$, respectively.

Further, the ionic conductivity of the polymer electrolytes were estimated by the equation $\sigma = L/RA$, where L, A and R are thickness, area and bulk resistance of the composite films, respectively. The bulk resistance was calculated from the high frequency intercept on the real impedance axis of the Nyquist plot [32]. The conductivity of the blank polymer electrolyte film was calculated to be $4.77 \times 10^{-4}\ S\,cm^{-1}$. However, the conductivity increased to $9.56 \times 10^{-4}\ S\,cm^{-1}$ for Co_3O_4 content of 1 wt.%. The commonly used perfluorosonic acid membrane Nafion® is known to have conductivity of $1.4 \times 10^{-2}\ S\,cm^{-1}$ [33]. Nevertheless, the conductivity obtained for the present composite is remarkable since, the conventionally used PEO based electrolytes have a significant drawback of low room temperature conductivity [2,4,34] and show satisfying ionic conductivity ($\sigma > 10^{-4}\ S\,cm^{-1}$) only at temperatures above 700 °C, when the polymer becomes amorphous. It is clear from the impedance study, that Co_3O_4 nanoparticles, indeed, make the conduction process easier between the solution and the electrode. Similar to ferrites, Co_3O_4 is a spinel having Co^{2+} and Co^{3+} ions in the lattice. In the presence of an applied electric field, $Co^{2+} \leftrightarrow Co^{3+}$ electronic exchange takes place which results in local displacement of charges. This behavior is similar to hopping conduction mechanism which is generally observed in ferrites. Moreover, as seen in Section 3.3, there is a decline in the crystalline phase of the polymer with the addition of Co_3O_4. The restriction of crystallization as well as the conduction process taking place in Co_3O_4 nanoparticles, collectively favor the improvement in conductivity.

4. Conclusion

PVDF/Co_3O_4 nanocomposite films were prepared by spin-coating technique. Electron microscopy micrographs showed aggregations of Co_3O_4 on the polymer surface which affected the porosity. An increase in magnetization values with increase in Co_3O_4 content indicated that the nanoparticles are well incorporated within the PVDF matrix. A decrease in porosity and crystallinity was observed with an increase in Co_3O_4 content. As a result, PVDF/Co_3O_4 system showed better conductivity, nearing the order $10^{-3}\ S\,cm^{-1}$, an order of magnitude higher than the blank PVDF film. These nanocomposite films can be exploited in the field of energy storage and electrochemical devices.

Acknowledgement

Financial assistance in the form of an R&D project grant from DST, Govt. of India is gratefully acknowledged. One of the authors, A.S. Bhatt, would like to thank NITK Surathkal for the award of research Fellowship.

Appendix A. Supplementary data

Supplementary data associated with this article can be found, in the online version, at doi:10.1016/j.mseb.2011.09.036.

References

[1] K.C. Ke, P. Strong, Polymer-nonionic Nanometer Composite Materials, Chemical Industry Publishing Company, Beijing, 2003.
[2] P. Lightfood, M.A. Mehta, P.G. Bruce, Science 262 (1993) 883–885.
[3] B. Kumar, L.G. Scanlan, J. Power Sources 52 (1994) 261–268.
[4] F. Croce, G.B. Appetacchi, L. Persi, B. Scrosati, Nature 394 (1998) 456–458.
[5] J.Y. Sang, Y.Y. Wang, C.C. Wan, J. Power Sources 77 (1999) 183–197.
[6] Y.J. Shen, M.J. Reddy, P.P. Chu, Solid State Ionics 175 (2004) 747–750.
[7] C.Y. Chiang, Y.J. Shen, M.J. Reddy, P.P. Chu, J. Power Sources 123 (2003) 222–229.
[8] N.S. Mohamed, A.K. Arof, J. Power Sources 132 (2004) 229–234.
[9] J.E. Dohany, L.E. Robb, Kirk–Othmer Encyclopedia of Chemical Technology, vol. II, 3rd ed., Wiley, New York, 1980, pp. 64–74.

[10] A.J. Lovinger, in: D.C. Basett (Ed.), Development in Crystalline Polymers, vol. 1, Applied Science, London, 1982, p. 195.
[11] Y.J. Wang, D. Kim, Electrochim. Acta 52 (2007) 3181–3189.
[12] J. Kulek, I. Szafraniak, B. Hilezer, M. Polomska, J. Non-Cryst. Solids 353 (2007) 4448–4452.
[13] R. Gregorio, M. Cestari, F.E. Bernardinio, J. Mater. Sci. 31 (1996) 2925–2930.
[14] A.S. Bhatt, D.K. Bhat, C.W. Tai, M.S. Santosh, Mater. Chem. Phys. 125 (2011) 347–350.
[15] Q. Shi, M.X. Yu, X. Zhou, Y.S. Yan, C.R. Wan, J. Power Sources 103 (2002) 286–292.
[16] J. Saunier, F. Alloin, J.Y. Sanchez, G. Caillon, J. Power Sources 119–121 (2003) 454–459.
[17] M. Hlavacek, J. Membr. Sci. 102 (1995) 1–7.
[18] K. Li, J.F. Kong, W.K. Teo, AlChE J. 45 (1999) 1211–1219.
[19] K. Schneider, T.S. Van Gasel, Chem. Eng. Technol. 56 (1984) 514.
[20] Y. Saito, A.M. Stephan, H. Kataoka, Solid State Ionics 160 (2003) 149–153.
[21] C.Y. Chiang, M.J. Reddy, P.P. Chu, Solid State Ionics 175 (2004) 631–635.
[22] C.W. Lin, C.L. Hung, M. Venketaswarlu, B.J. Hwang, J. Power Sources 146 (2005) 397–401.
[23] P. van de Witte, P.J. Dijkstra, J.W.A. van den Berg, J. Feijen, J. Membr. Sci. 117 (1996) 1–31.
[24] A.S. Bhatt, D.K. Bhat, M.S. Santosh, J. Appl. Polym. Sci. 119 (2011) 968–972.
[25] G. Wang, J. Roos, D. Brinkmann, F. Capuano, F. Croce, B. Scrosati, Solid State Ionics 53–56 (1992) 1102–1105.
[26] P.P. Chu, M.J. Reddy, J. Power Sources 115 (2003) 288–294.
[27] J.E. Weston, B.C.H. Steele, Solid State Ionics 7 (1982) 75–79.
[28] W. Wieczorek, K. Such, H. Wycilik, J. Pocharski, Solid State Ionics 36 (1989) 255–257.
[29] B. Kumar, S.J. Rodrigues, J. Electrochem. Soc. 148 (2001) A1336–A1340.
[30] T. Ambrose, C.L. Chein, Phys. Rev. Lett. 76 (1996) 1743–1746.
[31] R. Huq, G.C. Farrington, R. Koksban, P.E. Tonder, Solid State Ionics 57 (1992) 277–283.
[32] N.A. Choudhary, A.K. Shukla, S. Sampath, P. Pitchumani, J. Electrochem. Soc. 153 (2006) A614–A620.
[33] L.V.S. Lopes, D.C. Dragunski, A. Pawlicka, J.P. Donoso, Electrochim. Acta 48 (2003) 2021–2027.
[34] B. Kumar, L.G. Scanlon, J. Power Sources 52 (1994) 261–268.